



City Research Online

## City, University of London Institutional Repository

---

**Citation:** Vogiatzaki, K., Navarro-Martinez, S., De, S. & Kronenburg, A. (2015). Mixing modelling framework based on Multiple Mapping Conditioning for the prediction of turbulent flame extinction. *Flow, Turbulence and Combustion*, 95(2-3), pp. 501-517. doi: 10.1007/s10494-015-9626-0

This is the accepted version of the paper.

This version of the publication may differ from the final published version.

---

**Permanent repository link:** <https://openaccess.city.ac.uk/id/eprint/8130/>

**Link to published version:** <https://doi.org/10.1007/s10494-015-9626-0>

**Copyright:** City Research Online aims to make research outputs of City, University of London available to a wider audience. Copyright and Moral Rights remain with the author(s) and/or copyright holders. URLs from City Research Online may be freely distributed and linked to.

**Reuse:** Copies of full items can be used for personal research or study, educational, or not-for-profit purposes without prior permission or charge. Provided that the authors, title and full bibliographic details are credited, a hyperlink and/or URL is given for the original metadata page and the content is not changed in any way.

---

City Research Online:

<http://openaccess.city.ac.uk/>

[publications@city.ac.uk](mailto:publications@city.ac.uk)

---

# Mixing Modelling Framework Based on Multiple Mapping Conditioning for the Prediction of Turbulent Flame Extinction

K. Vogiatzaki<sup>1</sup> · S. Navarro-Martinez<sup>2</sup> · S. De<sup>3</sup> ·  
A. Kronenburg<sup>3</sup>

Received: 5 January 2015 / Accepted: 6 June 2015  
© Springer Science+Business Media Dordrecht 2015

**Abstract** A stochastic implementation of the Multiple Mapping Conditioning (MMC) approach has been applied to a turbulent piloted jet diffusion flame (Sandia flame F) that is close to extinction. Two classic mixing models (Curl's and IEM) are introduced in the MMC context to model the turbulent mixing. The suggested model involves the use of a reference space (that is mapped to mixture fraction space) in order to define particle proximity. The addition of the MMC ideas to the IEM and Curl's models, that is suggested in the current work, aspires to combine the simplicity of these two models with the enforced compositional locality without violating the linearity and independence principles. The formulation of the approach is discussed in detail and results are presented for the mixing field and reactive species. The predictions are compared with joint-scalar PDF simulations using the same mixing models and experimental data. Moreover, the sensitivity of the model to the particle number is examined. It is shown that MMC is less sensitive to the number of particles and can generally produce improved predictions of major and minor chemically reacting species with a lower number of particles.

---

✉ K. Vogiatzaki  
konstantina.vogiatzaki.2@city.ac.uk

S. Navarro-Martinez  
s.navarro@imperial.ac.uk

S. De  
santanu.de@itv.uni-stuttgart.de

A. Kronenburg  
kronenburg@itv.uni-stuttgart.de

<sup>1</sup> School of Engineering and Mathematical Sciences, City University, EC1V 0HB, London, UK

<sup>2</sup> Mechanical Engineering Department, Imperial College London, SW7 2AZ, London, UK

<sup>3</sup> Institut für Technische Verbrennung, University of Stuttgart, 70569, Stuttgart, Germany

22 **Keywords** Multiple mapping conditioning · Mixing models · Probability density function  
23 approach · Sandia flame F

## 24 1 Introduction

25 An important safety issue for engineers of combustion systems is the appearance of local  
26 extinction and re-ignition of the flame. These phenomena can be directly linked to the levels  
27 of turbulence in the combustion chamber. Overall, turbulence is a physical process highly  
28 desirable in combustion devices since it enhances the mixing of the fuel and oxidiser and  
29 accelerates the combustion process. However, due to its chaotic nature, small changes can  
30 result in a considerable increase of its intensity. If a critical value is exceeded very small  
31 eddies are generated that can penetrate the reaction zone reducing the flame temperature  
32 and disrupting the formation of radicals. Under these conditions the chemistry deviates  
33 from equilibrium and regions on the stoichiometric surface begin to extinguish. This could  
34 lead to global flame extinction or the flame may re-ignite depending on local strain-rate  
35 conditions.

36 Direct Numerical Simulation (DNS) would be the only numerical method capable of pro-  
37 viding a detailed description of extinction and re-ignition since burning and mixing occurs  
38 mostly at the smallest scales. However, due to the very large computing requirements Large-  
39 eddy (LES) and Reynolds averaged (RANS) simulations are the two alternative methods  
40 commonly used that involve some extra modelling. Although LES has drawn considerable  
41 attention of the academic community over the last decade, its application has not yet quite  
42 reached the industry sector. On the other hand RANS based CFD codes are still widely used  
43 in industries. In both, the RANS and LES contexts the instantaneous scalar dissipation –the  
44 term used to describe the levels of the mixing rate– is unclosed and thus the research around  
45 new turbulence combustion approaches that represent more accurately the mixing process  
46 is still very important.

47 The objective of the present work is to ascertain the capability of the Multiple Map-  
48 ping Conditioning (MMC) approach [21] and its closures to capture local extinction and  
49 re-ignition in laboratory flames in the RANS context. The MMC framework combines the  
50 probability density function (PDF) approach [27] and the mixture fraction based methods  
51 [20] via the application of a generalised mapping function to a prescribed reference space.  
52 PDF methods have been extensively applied to the modelling of turbulent reacting flows and  
53 a relatively recent comprehensive review is given by Haworth [14]. Of particular relevance  
54 are the studies by Pope and co-workers [3, 4, 36] where sensitivities of the PDF modelling  
55 approach towards parameters such as the mixing model [4], the mixing time scale [4] and  
56 the chemical mechanism [3] were investigated. Raman and Pitsch [30] successfully adapted  
57 the PDF methods as sub-grid scale model for large-eddy simulations. The Sandia flame  
58 series with flames of moderate to significant local flame extinction (Sandia Flames E and  
59 F) [1, 2] served as a test bed for all these modelling validation studies, and the same flames  
60 are used here for the validation of the MMC models.

61 With respect to the MMC modelling, stochastic and deterministic formulations exist, and  
62 both formulations have been explored in the past for the simple case of Sandia flame D [32,  
63 33], a flame with a relatively low degree of extinction. Variants of the original MMC for-  
64 mulation have been successfully applied to Sandia Flame E (and Flame F) using a hybrid  
65 binomial Langevin-MMC model for the modelling of the velocity-scalar interactions [35] or  
66 using a sparse particle method as sub-grid model for LES of the turbulent flow and mixing  
67 fields [12, 13]. In this work we focus exclusively on the stochastic implementation in the

RANS context, we base the MMC mixing model on the IEM and Curl's models (as opposed to IEM only that was used in earlier work [33]), we expand our study to the more challenging case of Sandia flame F, a flame with a relatively high Reynolds number and a considerable degree of extinction and re-ignition that has never been explored in the MMC context, and we assess the model dependence on the number of particles used for the stochastic solution of the composition field.

## 2 Turbulence-Chemistry Interaction Model

### 2.1 The PDF approach

Conventional PDF methods are based on the solution of the following equation that describes the evolution of the joint (one point) scalar PDF  $P = P(y, \mathbf{x}, t)$  of a set of  $n_s$  scalars  $Y_I$  ( $I = 1, \dots, n_s$ ).

$$\frac{\partial \langle \rho \rangle P_Y}{\partial t} + \nabla(\langle \rho \rangle u_Y P_Y) + \frac{\partial \langle \rho \rangle \langle \Omega | y \rangle P_Y}{\partial y_i} + \frac{\partial^2 \langle \rho \rangle N_{IJ} P_Y}{\partial y_i \partial y_j} = 0, \tag{1}$$

where  $u_Y$  is the conditional expectation of the flow velocity  $\mathbf{v}$  ( $u_Y(y, \mathbf{x}, t) = \langle \mathbf{v} | Y = y \rangle$ ) and  $N_{IJ}$  is the conditional scalar dissipation,  $N_{IJ} = \langle D \nabla Y_I \nabla Y_J | Y = y \rangle$ , which is by definition symmetric and positive semidefinite. The term  $D$  is the diffusion coefficient  $D_{IJ}$  (which is assumed to be the same for all species in high Reynolds number flows) and  $\Omega_I$  is the reaction rate.

The most commonly adopted approach to solving the above PDF evolution equation is the Lagrangian stochastic particle method, where the evolution of an ensemble of particles is used to represent the evolution of the (Eulerian) joint PDF of Eq. 1. In terms of implementation of the framework, a Lagrangian solver for the composition joint PDF is coupled with a standard Eulerian approach [14, 24, 25]. The solution domain in physical space is discretized into a number of cells for the purpose of extracting local mean quantities such as velocities which are then used in the particle evolution equations. Then, moments of reactive species, temperature and mixture fraction can be extracted by ensemble (or weighted) average of the particles in the same Eulerian cell. Properties of particles drawn from the same cell are considered to be local in the physical space. This approach is followed in the current work as well. Equation 1 is replaced by an equivalent set of stochastic differential equations of the following form

$$dx^* = (\mathbf{v}(x^*, t) + \frac{1}{\rho} \frac{\partial}{\partial \mathbf{x}}(\rho(D + D_t)))dt + \sqrt{2(D + D_t)}dw_i^*, \tag{2}$$

$$dY_I^* = [\Omega_I^* + S_I^*]dt. \tag{3}$$

The underlying idea is that the Fokker-Planck equation [11] that corresponds to the above set of equations has the same moments as those given by the PDF transport Eq. 1. Here and for the remainder of the paper, the superscript '\*' is used to distinguish the values linked to stochastic trajectories (stochastic particles), from deterministic quantities,  $D_t$  is the turbulent diffusivity and approximated by  $D_t \approx 0.09 * k^2/\epsilon/\sigma_t$  with  $\sigma_t = 0.7$  being the turbulent Schmidt number. Equation 2 accounts for transport in physical space while Eq. 3 accounts for transport in the composition space. The location of the particles is indicated as  $x^*$ ,  $w_i^*$  is a Wiener process with zero mean and variance equal to  $dt$  and  $S^*$  is a mixing operator that simulates the rate of change of scalar dissipation and in the Lagrangian particle context it represents (in a stochastically equivalent sense) the composition change of a fluid

107 particle under the effect of molecular mixing. The  $v(x^*, t)$  term is calculated by using the  
108 mean Eulerian velocity field  $v(x, t)$  interpolated to the particle position  $x^*$ .

109 For the modelling of  $S^*$  certain principles should be satisfied by the mixing models such  
110 as boundedness of the scalars, linearity of scalar transport, independence of the evolution  
111 of the particle properties and most importantly localness in the physical and compositional  
112 spaces [27, 31]. Treating fluid as continuum, molecular diffusion is an exchange of composi-  
113 tion between neighboring fluid particles which are infinitesimally close in both position and  
114 in composition. Although localness in the physical space is easy to impose in most models  
115 by allowing "mixing" among particles that belong to the same cell, localness in composition  
116 space is a major problem and much more difficult to impose [26]. Results [31] suggest that  
117 if particles mix with other particles in their immediate neighbourhood in composition space  
118 so that mixing across the reaction zone is avoided, the description of mixing is improved.  
119 On the contrary "artificial" extinction can be predicted for turbulent non-premixed flames  
120 at infinite Damköhler number if the principle of localness in composition space is violated.  
121 An additional difficulty is that in reality localness in the physical space and localness in the  
122 composition space in particle methods are two principles that interlink. In a recent study by  
123 [19] it is demonstrated that closeness in physical space can be related –in addition to local-  
124 ness in composition space– to the number of particles used in the calculations and of course  
125 to the resolution limitations originating from the resolution of the underlying Eulerian flow  
126 fields.

127 Different models have been suggested in the literature for  $S^*$ . Simple models that are  
128 easy to implement, such as the interaction by exchange with the mean (IEM) [10] and the  
129 various Curl's models [9, 16] do not ensure localness in the composition space. A more  
130 recent model, the Euclidean minimum spanning tree (EMST) [31] enforces locality but  
131 implementation is rather complicated, and it violates the linearity and independence princi-  
132 ples. A promising new model –the shadow-position mixing model (SPMM), was introduced  
133 in 2013 in [29] however up to date its applicability has only been demonstrated for the ide-  
134 alised case of a reactive scalar mixing layer. The addition of the MMC ideas to the IEM and  
135 Curl's model that is suggested in the current work and described in detail in the next sec-  
136 tion, aspires to combine the simplicity of these two models with the enforced compositional  
137 locality without violating the linearity and independence principles.

## 138 2.2 The MMC concept

139 MMC, by the use of a reference space, addresses some of the problems described in the  
140 previous section associated with the modelling of the mixing term. The basic idea of the  
141 mapping closure concept [5, 28] is to employ turbulent fluctuations and small-scale mixing  
142 in a mathematical reference space,  $\xi$ , with a known (or prescribed) PDF to model the mixing  
143 in the physical composition space with unknown PDF. A deterministic implementation of  
144 the method leads to closure of the conditional scalar dissipation [7, 17]. In the present  
145 paper, we focus on a stochastic implementation. If the reference space is chosen properly it  
146 can be used to enforce localness in composition space [21, 34]. The idea is to track particle  
147 position in the reference space and then allow mixing only among particles that are close to  
148 each other in  $\xi$ -space. Theoretically, events close in physical space should also be close in  
149 composition space, ensuring the localness of the MMC model.

150 The suggested approach can be considered to be an extension to the work of Wandel et  
151 al. [34] and has already been applied for the case of Sandia flame D using IEM as the only  
152 underlying mixing model [33]. It is a probabilistic MMC formulation with a single reference  
153 variable that is used to enforce localness in mixture fraction space and whose evolution

is described by a Markov process. MMC allows the choice of any number of reference variables, yet for flames with low levels of local extinction, localness in mixture fraction space is known to be sufficient to indicate localness in the multidimensional composition space. In a broader sense the shadow position model of [29] can be seen as a variation of the MMC concept where instead of enforcing locality through mixture fraction space, mixing is modeled as a relaxation of the composition to its mean conditional on the shadow position. In the present work we test if the enforced locality imposed by MMC can capture the behaviour of flames close to blow off.

We introduce a stochastic reference variable,  $\xi^*$ , which is governed by the following set of sdes

$$dx^* = U(\xi^*)dt, \tag{4}$$

$$d\xi^* = A^o dt + b^o dw^* \tag{5}$$

and for which we assume that the distribution is known.

The Fokker-Planck equation representing the above sde can be written as

$$\frac{\partial P_\xi}{\partial t} + \nabla U P_\xi + \frac{\partial A^o P_\xi}{\partial \xi} - \frac{\partial^2 B^o P_\xi}{\partial \xi^2} = 0, \tag{6}$$

where  $2B^o = (b^o)^2$ . Considering an arbitrary function of  $\xi^*$ ,  $f(\xi^*) = f^*$  a corresponding sde for this new random variable can be generated using an Ito transformation:

$$df(\xi^*) = \tilde{A}dt + \tilde{b}dw^*, \tag{7}$$

with

$$\tilde{A} = \frac{\partial f(\xi)}{\partial t} + U \nabla f(\xi) + \left( A^o \frac{\partial f(\xi)}{\partial \xi} + B^o \frac{\partial^2 f(\xi)}{\partial \xi^2} \right) \tag{8}$$

and

$$\tilde{b} = b^o \frac{\partial f(\xi)}{\partial \xi} \tag{9}$$

The Fokker Planck equation representing the above sde is given by

$$\frac{\partial P_f}{\partial t} + \nabla U P_f + \frac{\partial \tilde{A} P_f}{\partial f} - \frac{\partial^2 \tilde{B} P_f}{\partial f^2} = 0. \tag{10}$$

The advantage of the “mapping” is that by assuming a shape for  $P_\xi$  we can define  $A^o$  and  $b^o$  from Eq. 6. We can then define the unknown drift and diffusion coefficients for the new stochastic process  $f(\xi^*)$  and consequently the evolution of its PDF. It should be noted that the equivalent PDF describes the one-point one-time cell distribution. A two-point strategy has been suggested based on mapping functions that incorporate two-points statistics [15] however it has not been attempted here.

Following the probabilistic approach and adding to the equations for a standard PDF approach, Eqs. 2 and 3, the two new MMC equations, Eqs. 5 and 7, that embody the mapping closure concept, the general probabilistic approach gives

$$dx^* = U(\xi^*)dt, \tag{11}$$

$$d\xi^* = A^o dt + b^o dw^*, \tag{12}$$

$$d\bar{Y}(\xi^*) = \tilde{A}dt + \tilde{b}dw^*, \tag{13}$$

$$dY^* = [\Omega_I^* + S_I^*]dt. \tag{14}$$

It should be noticed that Eq. 13 is not solved since it is in reality equivalent to Eq. 12. This mathematical equivalence is the key that explains the concept that an appropriate choice of the reference space will also guarantee localness in composition space. To keep

187 the computational cost low, the reference variables generate the fluctuations of a selected  
 188 number of species only (the so called “major species”) and the fluctuations of the remaining  
 189 species (the so called “minor species”) are linked to the fluctuations of major species similar  
 190 to the conditional moment closure methodology [21]. Thus, it is only necessary to establish  
 191 mapping relations as Eq. 13 for the major species and this is here mixture fraction,  $Z$ . For  
 192 each major species that has a corresponding reference variable, the MMC transport equation  
 193 becomes a PDF transport equation [21], [18]. Thus,  $A^o$ ,  $B^o$  and  $U(\xi^*)$  must be chosen so  
 194 that  $\tilde{A}$  and  $\tilde{B}$  describe a diffusion process for mixture fraction. If we assume a Gaussian  
 195 distribution for the reference variable and equate Eqs. 10 to 1 for mixture fraction we can  
 196 obtain the unknown coefficient  $A^o$  and  $b^o$  from

$$\mathbf{U} = \mathbf{U}(\xi; \mathbf{x}, t) = \mathbf{U}^{(0)} + \mathbf{U}^{(1)}\xi, \tag{15}$$

$$A^o = -\frac{\partial B^o}{\partial \xi} + B^o\xi + \frac{1}{\langle \rho \rangle} \nabla \langle \rho \rangle \mathbf{U}^{(1)} + \frac{2}{P_\xi} \frac{\partial B^o P_\xi}{\partial \xi}, \tag{16}$$

$$\mathbf{U}^{(0)} = \langle v \rangle, \tag{17}$$

$$\mathbf{U}^{(1)} \langle \xi Z \rangle = \langle v' Z' \rangle. \tag{18}$$

200 The turbulent flux can be modelled by a standard gradient approximation,  $\langle v' Z' \rangle =$   
 201  $-D_t \nabla \langle Z \rangle$  and  $\langle \xi Z \rangle$  results directly from the solution of  $Z(\xi)$  (c.f Fig. 1). The term  
 202  $B^o$  is modelled independently of  $\xi$ ,  $B^o = B^o(\mathbf{x}, t)$ , and is related to the scalar dissipation  
 203  $\langle N_Z \rangle$  through

$$B^o \left\langle \left( \frac{\partial Z}{\partial \xi} \right)^2 \right\rangle = \langle N_Z \rangle. \tag{19}$$

204 It is apparent from Eq. 19 that closure of the MMC model requires knowledge of the  
 205 unconditional scalar dissipation of  $Z$ , but it does not explicitly include the more difficult  
 206 to model conditional scalar dissipation. The dissipation  $\langle N_Z \rangle$  can be modelled adopting  
 207 Corrsin’s suggestion [8] that the decay rate of a passive scalar variance is assumed to be  
 208 proportional to the decay rate of the turbulent kinetic energy i.e.

$$\langle N_Z \rangle = 0.5 \frac{\langle Z'^2 \rangle}{\tau_D}, \tag{20}$$

209 where  $\tau_D$  is proportional to the flow turbulent time scale  $\tau = k/\varepsilon$  with a proportionality  
 210 constant commonly assumed to be  $C_D = 1/C_\phi = 0.5$ .

211 It should be noted that three different definitions of fluctuations exist in MMC: the  
 212 unconditional fluctuations or major fluctuations  $Y_I' = Y_I - \langle Y_I \rangle$ , the minor fluctuations  
 213  $Y_I'' = Y_I - \langle Y_I | \xi \rangle$  and the fluctuations around a quantity, conditionally averaged on mixture  
 214 fraction itself,  $Y_I''' = Y_I - \langle Y_I | Z \rangle$ . The diffusion coefficient  $B^o$  controls the major fluctu-  
 215 ations while the mixing operator  $S_I^*$  controls the minor fluctuations. In the current work  
 216 two different models have been implemented which are essentially modified versions of the  
 217 well known IEM and Curl’s model.

218 When using the modified IEM model (MMC-IEM) the particles are mixed with their  
 219 means conditioned on a certain value in the reference space  $\langle Y_I | \xi \rangle$

$$S_I^* = \frac{1}{2} \frac{\overline{Y_I}(\xi^*) - Y_I^{*p}}{\tau_{min}}. \tag{21}$$

220 For the modified version of the Curl’s model (MMC-Curl’s) at each time step all particles  
 221 that belong to the same Eulerian cell are formed into pairs and mix with their mean. The  
 222 selection of every particle pair is not random as in commonly used Curl’s models but it is



according to the distance of the particles in the reference space. For the present work, only particles that belong to the same  $\xi$ -bin are allowed to mix following

$$S_I^* = \frac{1}{2} \frac{0.5(Y_I^{*p} + Y_I^{*q}) - Y_I^{*p}}{\tau_{min}}, \tag{22}$$

with  $\langle S^*|\xi^*, x^* \rangle = 0$  [21]. The simplicity of both models is attractive for implementation, but the estimation of the “minor dissipation time”,  $\tau_{min}$ , is rather problematic since minor fluctuations exist only in the context of MMC. Wandel and Klimenko [34] used DNS of homogeneous turbulence to obtain a time scale ratio between the minor and major dissipation time of  $\tau_{min}/\tau_D = 1/8$ . However, Vogiatzaki et al. [33] could not corroborate these findings for laboratory jet diffusion flames. Mixing time scales smaller than  $\tau_D$  were found to suppress most minor fluctuations and lead to a significant underprediction of the conditionally averaged variances. For Sandia Flame D, best results were obtained with  $\tau_{min} = \tau_D$ , and this value is adopted here.

### 3 Computational Methods

The test case (Sandia flame F) [1] consists of a methane/air fuel mixture that issues from a central  $d = 7.2\text{mm}$  internal diameter nozzle surrounded by a coaxial pilot flame with an outer diameter of  $18.2\text{mm}$ . The fuel is 25 %  $CH_4$  and 75 % air by volume with a stoichiometric mixture fraction of  $Z_{st} = 0.351$ . The jet Reynolds number is 44,800, the pilot inlet velocity is  $22.8\text{m/s}$  and the velocity of the co-flowing air is  $0.9\text{m/s}$ .

The PDF approach is used in order to model the turbulence-chemistry interaction. The composition PDFs are calculated by Monte Carlo methods, while a finite-volume method was applied to solve for the mean velocity, dissipation, and mean pressure fields. The Eulerian flow field equations are solved using an in-house RANS code (BOFFIN). Turbulence is modelled by a standard  $k-\epsilon$  model [23]. A cylindrical domain extends  $0.65\text{m}$  in downstream direction and  $0.15\text{m}$  in radial direction and is discretised by 200 axial and 100 radial finite volume cells. An augmented reduced mechanism (ARM2) derived from the full GRI 3.0 mechanism using quasi-steady assumptions for some minor species is incorporated to describe the chemical reactions [6]. Cao and Pope [3] demonstrated that ARM2 is capable of predicting the correct extinction levels for all Sandia Flames D-F but for flame F, results may be sensitive towards small changes in the boundary conditions or modelling parameters. For the composition field calculations, three different particle densities have been used in order to assess the sensitivity of the models on particle number. The different test cases are listed in Table 1. The evolution of the particle properties is modelled by Eqs. 11 to 14. We emphasise that every particle carries information on its (stochastic) velocity, species concentration, temperature and reference space  $\xi$ , obtained from Eq. 12.

Note that the reference space is Gaussian and unbounded, but the deterministic drift term counteracts the random diffusion term and keeps particles close to the mean. Then

**Table 1** Overview of the test cases with corresponding number of particles

Test case	Number of Particles	Particles per cell
1	400.000	20
2	1.000.000	50
3	2.000.000	100

259 depending on their  $\xi$  value the particles within each cell are ordered in the reference sample  
 260 space that extends from -4 to 4, divided into 16  $\xi$ -bins. In each  $\xi$ -bin,  $\langle Y_I | \xi \rangle$  is defined by an  
 261 ordinary averaging process. For empty  $\xi$ -bins, values are obtained from linear interpolation.

262 It is important to emphasize that the calculations with 20 particles/cell take 5 hours on  
 263 a single core machine. The computational cost is tripled when the number of particles is  
 264 increased to 100 particles per cell. Previous Lagrangian PDF approaches in the RANS con-  
 265 text use a wide range of particle numbers (from 100 particles/cell [36] to 800 particles/cell  
 266 [24]). Although the absolute computational time depends on the specific characteristic of  
 267 the codes used in these calculations, it is obvious that a significant increase of the num-  
 268 ber of particles will significantly increase the computational cost. This increase can be very  
 269 important for the calculation of a realistic industrial geometry with a considerably bigger  
 270 grid. Thus, a very desirable characteristic of any new mixing model is to perform well with a  
 271 relatively low number of particles per cells. This motivated the three numerical experiments  
 272 with different numbers of particles

273 **4 Results and Discussion**

274 Figure 1 is a graphic representation of the MMC concept at  $x/d = 15$  at three radial locations  
 275 of the flame under consideration: on the rich side ( $r/d = 0.1$ ), in the shear layer ( $r/d = 1$ )  
 276 and on the lean side ( $r/d = 2$ ). As mentioned above every particle carries a set of values that  
 277 represent its (stochastic) velocity, species concentration, temperature *and*  $\xi$ . This creates a  
 278 correlation between temperature, (or any reactive species), mixture fraction and reference

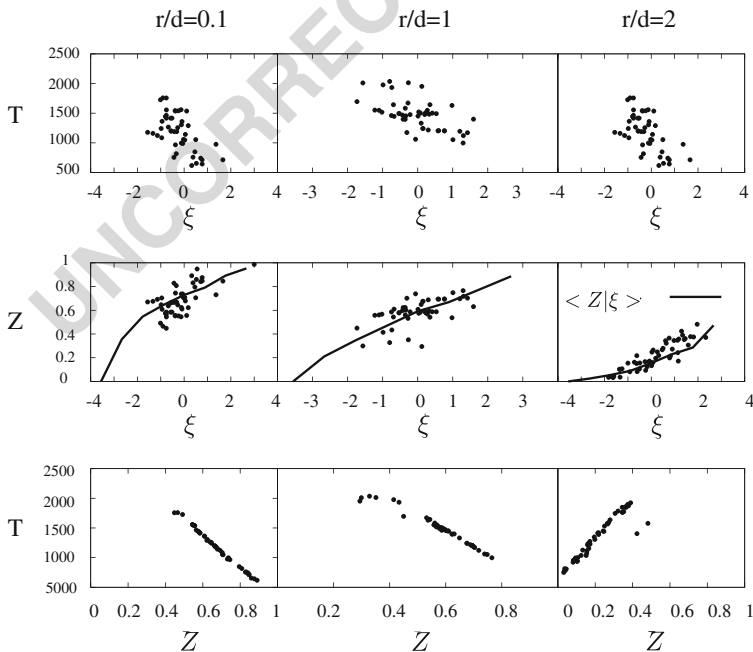


**Fig. 1** MMC mapping concept: *first row* – temperature versus reference space at three radial locations; *second row* – computed mapping function; *third row* – temperature versus mixture fraction for the MMC-IEM mixing model

space which is demonstrated in the top two rows of the figure. Closeness of the particles in the reference space controls closeness of the particles in the mixture fraction space and consequently in the temperature (or composition) space as can be seen in the figures in the bottom row. This correlation exists only because the evolution of the reference space, Eq. 12, is not independent of the evolution of the species, Eq. 13. Consequently, mixing particles that are close in reference space is equivalent to mixing particles close in composition space. It is important to stress that if the particle's value of the reference space was held constant throughout the calculations, the reference variable and mixture fraction would decorrelate with time (or distance from the jet exit) and the method would collapse to a conventional PDF approach. The decorrelation would be equivalent to horizontal lines of the averaged mixture fraction,  $\langle Z | \xi \rangle$ , in the middle row of Fig. 1.

In Fig. 2 the radial profiles of the mean and root mean square (rms) of the mapping function (mixture fraction) are presented for all four mixing models, IEM, MMC-IEM, Curl's and MMC-Curl's. It is apparent that the mixing field is quite insensitive to the choice of the mixing model. The simulations presented in this figure are performed with 20 particles/cell, the quality of predictions for test cases 1 to 3 (see Table 1) is comparable for all models and none of them shows a significant dependence on the particle number. As it has been shown in previous studies [4, 36] the predictions for the mixture fraction depend mostly on the choice of the mixing time scale that for the current work is the same for all four models.

Figures 3, 4, 5 and 6 show the scatter plots of temperature at different axial locations for three different particle loadings. Figure 7 shows the experimental results and serves as comparison. These figures allow a qualitative assessment, and MMC (both with IEM and Curl's), yields a somewhat more realistic scatter in temperature with fewer realizations above equilibrium conditions than the classic models. The MMC-IEM model is not capable of fully capturing the extent of extinguished flame elements as seen in the experiments, but it needs to be emphasized here that MMC-IEM provides qualitatively reasonable predictions even with a very small number of particles. These results should be compared with

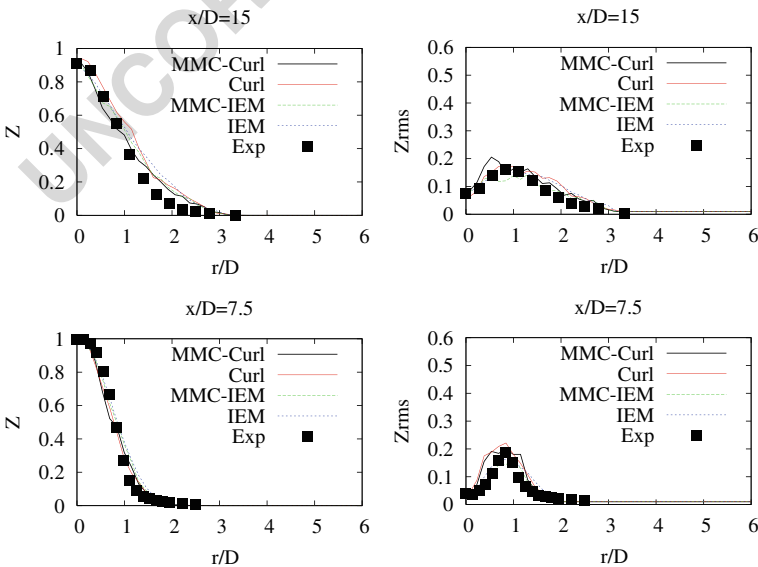


**Fig. 2** Radial profiles of mean (left) and rms (right) of mixture fraction  $Z$  at different axial locations

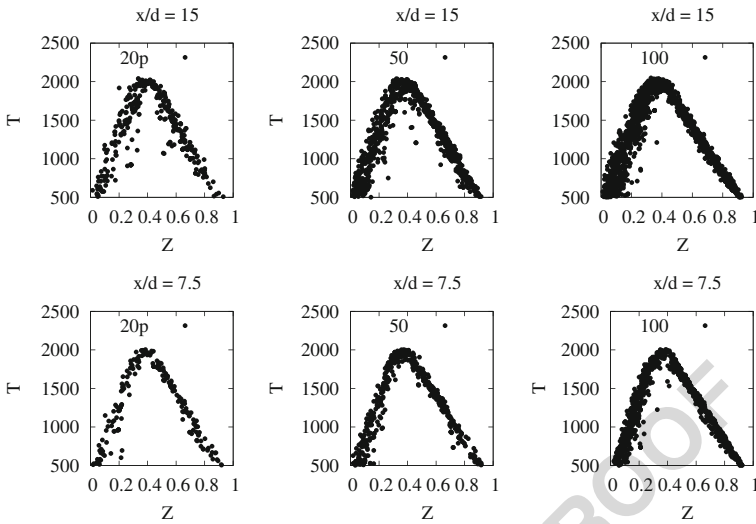


**Fig. 3** MMC-IEM: scatter plots of temperature at different axial locations and for different particle number densities

306 conventional IEM simulations (see Fig. 4). The IEM mixing model creates two very distinct  
 307 branches, one burning and one non-burning, that are not present in Fig. 7 and yield an  
 308 unphysical bias towards certain realizations in composition space. Note that the computa-  
 309 tion of the mean value in the cell, used for the mixing model, is based on the instantaneous  
 310 cell population and it slightly varies with the iteration and is thus dependent on the number

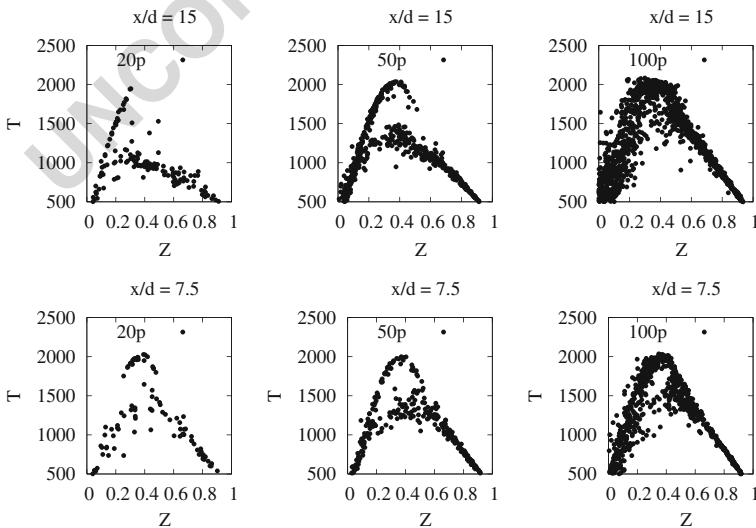


**Fig. 4** IEM: Scatter plots of temperature at different axial locations and for different particle number densities

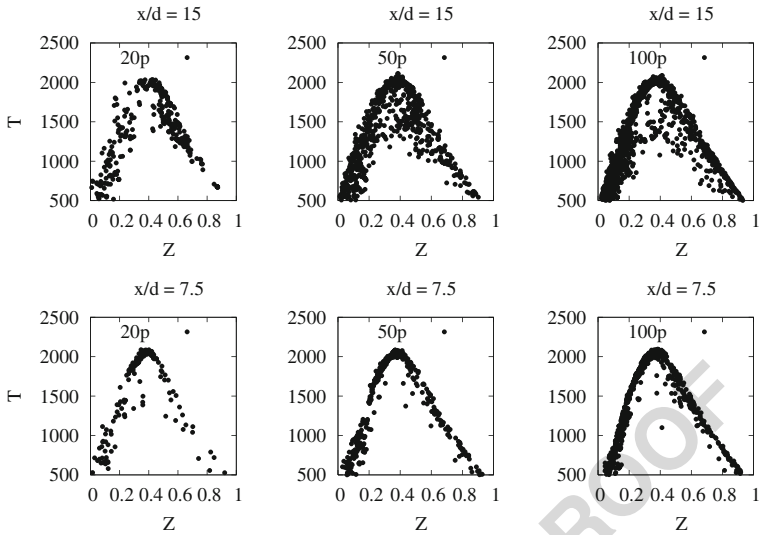


**Fig. 5** MMC-Curl's: Scatter plots of temperature at different axial locations and for different particle number densities

of the particles in the cell. The dependence of the IEM model on particle number would 311  
vanish if averages over many iteration would be used instead. 312

The MMC-Curl's model appears to provide the best qualitative agreement with the exper- 313  
imental data especially further downstream. The conventional Curl's model also predicts 314  
the extinction satisfactorily, but some spurious behaviour can be observed especially on the 315  
lean side when only few particles are used. The reader should note that we have used the 316

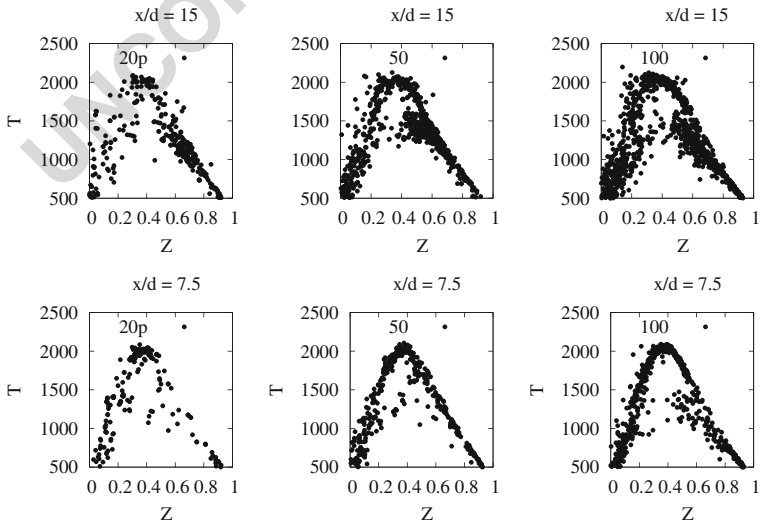


**Fig. 6** Curl's: Scatter plots of temperature at different axial locations and for different particle number densities

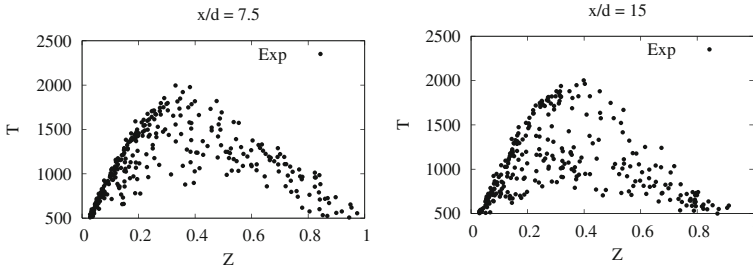


**Fig. 7** Experiment: Scatter plots of temperature at different axial locations

317 simple Curl’s model in its original form and not its modified version. No additional control  
 318 of the mixing process to limit unphysical super-equilibrium values has been attempted.

319 A better insight is provided by Figs. 8 and 9. Here, the radial profiles of the conditional  
 320 temperature and its conditional rms at different axial locations are presented and the MMC-  
 321 IEM and IEM models can be compared. It can be clearly seen that IEM shows a strong  
 322 dependence on the particle number while MMC-IEM is much less sensitive to particle den-  
 323 sity and only 20 particles per cell yield an independence of the solution from the particle  
 324 density while IEM requires around 100 particles/cell to approximate the same results. The  
 325 conditional rms are considerably under-predicted for the MMC-IEM and the IEM model  
 326 appears to be somewhat better. However these predictions should be always viewed in con-  
 327 junction with Figs. 3 and 4. The high rms values result from unphysical mixing of particles  
 328 that create two distinct burning modes rather than a uniform scattering as the one seen in  
 329 the experiments (see Fig. 7).

330 These trends are similar but much less pronounced for MMC-Curl’s and Curl’s model  
 331 (not shown here). MMC-Curl’s and Curl’s yield conditional temperatures closer to the  
 332 experimental values at both axial locations, and the classic Curl’s mixing model is only

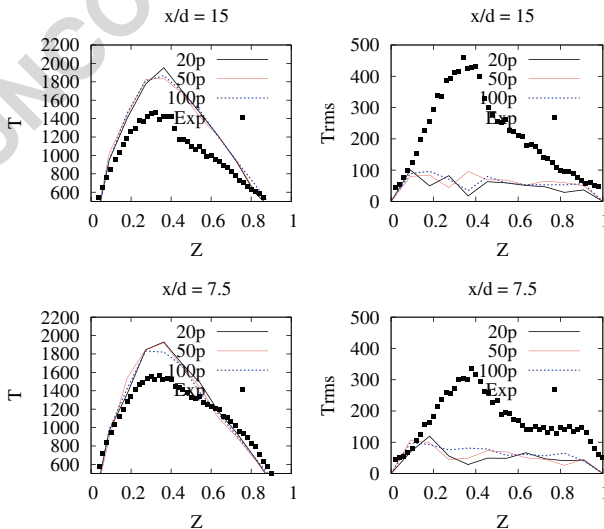


**Fig. 8** Radial profiles of conditional temperature and rms at different axial locations with MMC-IEM

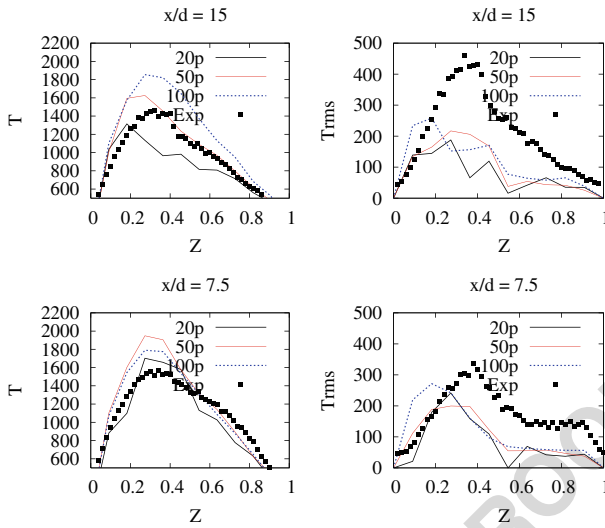


**Fig. 9** Radial profiles of conditional temperature and rms at different axial locations with IEM

slightly more sensitive to the particle number density than MMC-Curl's. The better agreement with experimental data can be attributed to the fact that pair-wise models are known to model mixing more realistically than mean based models. It is emphasized again, that for all test cases the same mixing constant has been used, and no efforts have been made to control mixing through the mixing time scale as is a common practice. This does not necessarily imply that all the models have the best performance with the same constant. Adjustments of the mixing constant  $C_\phi$  could have led to more realistic degrees of extinction and can have effects on the stability of the numerical solution but may deteriorate the mixing field predictions [4] and would not aid the analysis of the differences between MMC-enhanced mixing models and the particle number dependence.

The predictions of the radial profiles of temperature (not shown here) are generally less sensitive to the number of particles for all models and the same holds for species such as  $\text{CH}_4$ . It can be noticed that for all the test cases the temperature predictions are satisfying and a small improvement is noticed with the addition of MMC for radial positions  $r/d > 1.5$  (towards the lean side of the flame). On the other hand the prediction of species such as CO or  $\text{H}_2\text{O}$  that are more sensitive to small changes of temperature is more challenging and more dependent on the quality of the mixing model. Figures 10 and 11 show the radial profiles of CO at different axial locations. MMC shows less sensitivity to the particle number when compared to IEM and less noise than Curl's, which indicates increased numerical stability that was reported to be an issue in earlier PDF calculations when using IEM and Curl's mixing models [4, 36]. MMC-Curl's with 100 particles/cell gives the overall best agreement.

IEM and MMC-IEM have opposite tendency when the particle number is increased at  $x/d=15$ ; the more particles are used in IEM, the higher the temperature, re-igniting the flame. This is consistent with the scatter plot in Fig. 4 where the lower branch disappears as the number of particles increases. MMC-IEM have a much more uniform behaviour, with minimum difference in temperature predictions with particle refinement. Doubling the number of particles barely decreases the peak temperature by 50 K. The particle dependence of IEM

333  
334  
335  
336  
337  
338  
339  
340  
341  
342  
343  
344  
345  
346  
347  
348  
349  
350  
351  
352  
353  
354  
355  
356  
357  
358  
359  
360

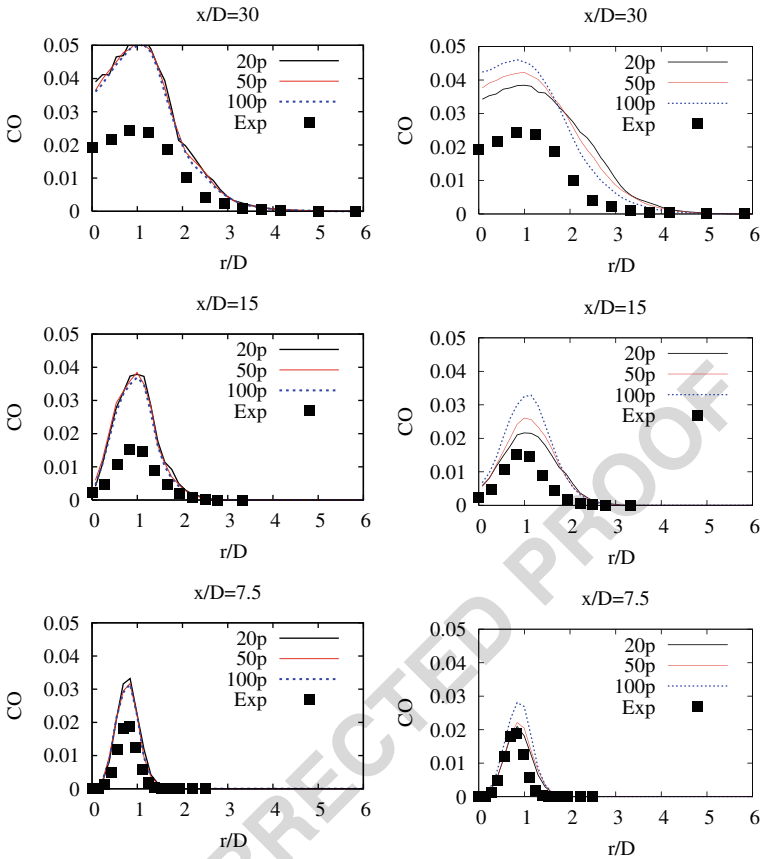


**Fig. 10** Radial profiles of CO at different axial locations with MMC-IEM (left) IEM(right)

361 is amplified, when we look at CO predictions (see Fig. 10) at  $x/d=15$ . At the same position  
 362 the MMC-IEM shows no particle number dependency, although it under-predicts extinction  
 363 as observed in Fig. 8.

364 When the Curl's mixing sub-model is used, both MMC-Curl's and Curl's exhibit large  
 365 particle dependency in and around the zone with significant extinction (see Fig. 11). This  
 366 suggests that when extinction occurs, large numbers of particles per cell are indeed needed.  
 367 However, away from it, fewer particles per cell are needed in the MMC context as the  
 368 extra dependence on the reference space improves the mixing description. Probably more  
 369 than one reference space is needed when severe extinction occurs, a modification suggested  
 370 in previous studies as well [7, 22]. In the case of Curl's, large fluctuations are observed  
 371 even with 100 particles per cell, while MMC produces smoother statistics. This can be  
 372 easily understood by the nature of the corresponding SDE's of the MMC and PDF methods,  
 373 Eqs. 13 and 2, respectively. The diffusion coefficient of MMC equations can be zero locally,  
 374 unlike the PDF equations, and therefore statistical noise can be globally reduced.

375 An additional observation is that MMC shows better behaviour along the centreline and  
 376 this is probably due to a better numerical treatment of the conditional velocity close to the  
 377 centreline. It is not in the scope of this paper to explore the modelling of the conditional



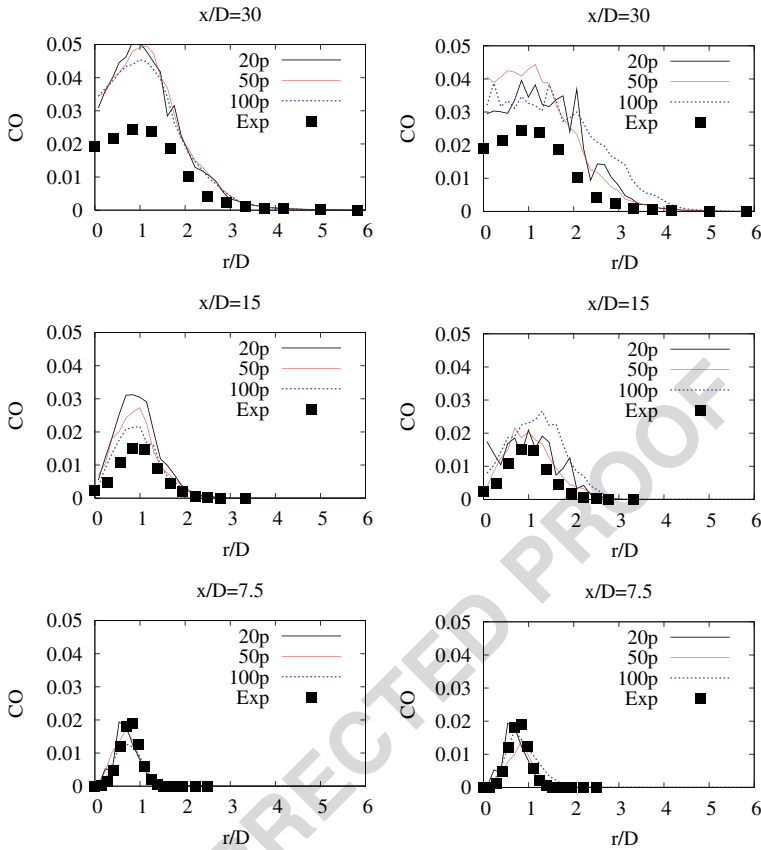


**Fig. 11** Radial profiles of CO at different axial locations with MMC-Curl's (left) Curl's (right)

velocity, however, it can be briefly noticed from Eq. 15 and 18 that the fluctuating part of the velocity becomes zero when the gradients of mixture fraction are zero allowing particles to follow the mean flow field trajectories.

**5 Conclusion**

In this paper we suggest a numerical framework for modelling the mixing term of the joint-scalar PDF. Two models are tested for the prediction of the degree of extinction of a piloted non-premixed turbulent methane flame close to blow off. The behaviour of two new mixing models has been assessed in the MMC context and compared to common mixing models in the literature. The models suggested in this work are extensions of two classic mixing models (Curl's and IEM) and aspire to overcome the deficiencies of the classical models modelling of flames close to extinction. The results indicate that by introducing to the Curl's and IEM model indirect localness in the mixture fraction space through the use of the reference space, the predictions' sensitivity to the number of particles is reduced. This trend is more pronounced for the MMC-IEM variation of the model. For all test cases no efforts have been made to control mixing through the mixing time scale as is a common practice

393 and the same constant was used. Although it is well known that adjustments of the mixing  
394 constant  $C_\phi$  could have led to more realistic degrees of extinction this would diminish the  
395 assessment of the predictive capabilities of the MMC-enhanced mixing models in terms of  
396 particle number dependence.

397 **Acknowledgments** Support is acknowledged from Deutsche Forschungsgemeinschaft (DFG) under grant  
398 number KR3684/7-1. Dr Vogiatzaki would like to acknowledge the contribution of The Lloyds Register  
399 Foundation. Lloyds Register Foundation helps to protect life and property by supporting engineering-related  
400 education, public engagement and the application of research.

## 401 References

- 402 1. Barlow, R., Frank, J.: Effects of turbulence on species mass fractions in methane/air jet flames. Proc.  
403 Combust Inst **27**, 1087–1095 (1998)
- 404 2. Barlow, R., Frank, J., Karpetis, A., Chen, J.Y.: Piloted methane/air jet flames: Transport effects and  
405 aspects of scalar structure. Combust. Flame **143**, 433–449 (2005)
- 406 3. Cao, R., Pope, S.: The influence of chemical mechanisms on pdf calculations of nonpremixed piloted jet  
407 flames. Combust. Flame **143**, 450–470 (2005)
- 408 4. Cao, R., Wang, H., Pope, S.: The effect of mixing models in pdf calculations of piloted jet flames. Proc.  
409 Combust Inst **31**, 1543–1550 (2007)
- 410 5. Chen, H., Chen, S., Kraichnan, R.: Probability distribution of a stochastically advected scalar field. Phys.  
411 Rev. Lett. **63**(24), 2657–60 (1989)
- 412 6. Sung, C.J., Law, C., Chen, J.: Augmented reduced mechanisms for no emission in methane oxidation.  
413 Combust. Flame **125**(1–2), 906–919 (2001)
- 414 7. Cleary, M., Kronenburg, A.: Hybrid multiple mapping conditioning on passive and reactive scalars.  
415 Combust. Flame **151**(4), 623–638 (2007)
- 416 8. Corrsin, S.: J. Aeronaut. Sci. **18**, 417 (1951)
- 417 9. Curl, R., Miller, R., Ralph, J., Towell, G.: Dispersed phase mixing: Ii. measurements in organic dispersed  
418 systems. AIChE J. **9**, 175–181 (1963)
- 419 10. Dopazo, C.: Probability density function approach for a turbulent heated jet. centerline evolution. Phys.  
420 Fluids **18**, 397–404 (1975)
- 421 11. Gardiner, C.: Handbook of stochastic methods. Springer, New York (1984)
- 422 12. Ge, Y., Cleary, M., Klimenko, A.: Sparse-lagrangian {FDF} simulations of sandia flame e with density  
423 coupling. Proc. Combust. Inst. **33**(1), 1401–1409 (2011)
- 424 13. Ge, Y., Cleary, M., Klimenko, A.: A comparative study of sandia flame series (df) using sparse-  
425 lagrangian {MMC} modelling. Proc. Combust. Inst. **34**(1), 1325–1332 (2013)
- 426 14. Haworth, D.: Progress in probability density function methods for turbulent reacting flows. Prog. Energy  
427 Combust. Sci. **36**, 168259 (2010)
- 428 15. He, G.W., Zhang, Z.F.: Two-point closure strategy in the mapping closure approximation approach. Phys.  
429 Rev. E **70**(036), 309 (2004)
- 430 16. Janicka, J., Kolbe, W., Kollmann, W.: Closure of the transport equation for the probability density  
431 function of turbulent scalar fields. J. Nonequil. Thermodyn **4**, 47–66 (1979)
- 432 17. Klimenko, A.: Modern modelling of turbulent non-premixed combustion and reaction of pollution  
433 emission. Proceedings of Clean Air VII, Lisbon, Portugal (2003)
- 434 18. Klimenko, A.: Matching the conditional variance as a criterion for selecting parameters in the simplest  
435 multiple mapping conditioning models. Phys. Fluids **16**(12), 4754–4757 (2004)
- 436 19. Klimenko, A.: On simulating scalar transport by mixing between lagrangian particles. Phys. Fluids **19**(3),  
437 31,702 (2007)
- 438 20. Klimenko, A., Bilger, R.: Conditional moment closure for turbulent combustion. Prog. Energy Combust.  
439 Sci **25**(6), 595–687 (1999)
- 440 21. Klimenko, A., Pope, S.: The modeling of turbulent reactive flows based on multiple mapping condition-  
441 ing. Phys. Fluids **15**(7), 1907–1925 (2003)
- 442 22. Kronenburg, A., Cleary, M.J.: Multiple mapping conditioning for flames with partial premixing.  
443 Combust. Flame **155**, 215–231 (2008)
- 444 23. Launder, B., Spalding, D.: The numerical computation of turbulent flows. Comput. Methods Appl. Mech.  
445 Eng. **3**(2), 269–289 (1974)

24. Lindstedt, R., Louloudi, S., Vaos, E.M.: Joint scalar probability density function modeling of pollutant formation in piloted turbulent jet diffusion flames with comprehensive chemistry. *Proc. Combust Inst* **28**(1), 149156 (2000) 446  
447
25. Muradoglu, M., Jenny, P., Pope, S.B., Caughey, D.A.: A consistent hybrid finite-volume/particle method for the pdf equations of turbulent reactive flows. *J. Comp. Phys.* **154**, 342371 (1999) 449  
450
26. Norris, A., Pope, S.: Turbulent mixing model based on ordering pairing. *Combust. Flame* **83**(1–2), 27–42 (1991) 451  
452
27. Pope, S.: PDF methods for turbulent reactive flows. *Prog. Energy Combust. Sci.* **11**(2), 119–192 (1985) 453
28. Pope, S.: Mapping closures for turbulent mixing and reaction. *Theor. Comput. Fluid Dyn* **2**(5–6), 255–70 (1991) 454  
455
29. Pope, S.B.: A model for turbulent mixing based on shadow-position conditioning. *Phys. Fluids* **25**(11) (2013) 456  
457
30. Raman, V., Pitsch, H.: A consistent les/filtered-density function formulation for the simulation of turbulent flames with detailed chemistry. *Proc Combust Inst* **31**, 1711–1719 (2007) 458  
459
31. Subramaniam, S., Pope, S.: A mixing model for turbulent reactive flows based on euclidean minimum spanning trees. *Combust. Flame* **115**(4), 487–514 (1999) 460  
461
32. Vogiatzaki, K., Cleary, M., Kronenburg, A., Kent, J.: Modeling of scalar mixing in turbulent jet flames by multiple mapping conditioning. *Phys. Fluids* **21**(2) (2009) 462  
463
33. Vogiatzaki, K., Kronenburg, A., Navarro-Martinez, S., Jones, W.: Stochastic multiple mapping conditioning for a piloted, turbulent jet diffusion flame. *Proc. Combust Inst* **33**(1), 1523–1531 (2011) 464  
465
34. Wandel, A., Klimenko, A.: Testing multiple mapping conditioning mixing for monte carlo probability density function simulations. *Phys. Fluids* **17**(12), 128,105 (2005) 466  
467
35. Wandel, A.P., Lindstedt, R.P.: Hybrid multiple mapping conditioning modeling of local extinction. *Proc. Combust. Inst.* **34**(1), 1365–1372 (2013) 468  
469
36. Xu, J., Pope, S.B.: Pdf calculations of turbulent nonpremixed flames with local extinction. *Combust. Flame* **123**(3), 281–307 (2000) 470  
471

UNCORRECTED PROOF

**AUTHOR QUERY**

No Query.